

# On the Dehalogenation Mechanism of 4-Chlorobenzoyl CoA by 4-Chlorobenzoyl CoA Dehalogenase: Insights from Study Based on the Nonenzymatic Reaction

Ya-Jun Zheng and Thomas C. Bruice\*

Contribution from the Department of Chemistry, University of California at Santa Barbara, Santa Barbara, California 93106

Received January 15, 1997<sup>⊗</sup>

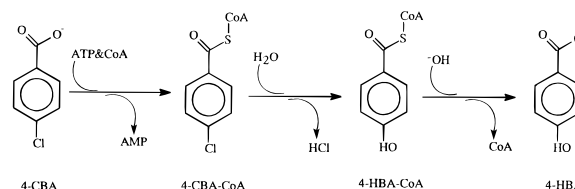
**Abstract:** The conversion of 4-chlorobenzoate to 4-hydroxybenzoate is carried out by first esterifying 4-chlorobenzoate by coenzyme A, and the resulting 4-chlorobenzoyl CoA serves as substrate for the 4-chlorobenzoyl CoA dehalogenase. To gain a better appreciation of the catalytic mechanism and factors controlling the catalytic efficacy of this dehalogenase, the nucleophilic aromatic substitution reaction between 4-Cl-Ph-CO-SCH<sub>3</sub> and CH<sub>3</sub>COO<sup>-</sup> was investigated in detail in both gas phase and solution (the -CH<sub>2</sub>COO<sup>-</sup> entity of Asp145 is the enzyme nucleophile). Quantum mechanical methods (HF/6-31G\*, B3LYP/6-311+G\*\*, and PM3) were used to elucidate the gas phase reaction. The gas phase reaction profile is best described as a two-well potential surface, with the two minima corresponding to reactant-side and product-side ion–molecule complexes. There is a small overall potential energy barrier, but the free energy barrier is significant. On the HF/6-31G\* potential energy surface, no minimum corresponding to the Meisenheimer intermediate was found; however, there is a shallow one on the PM3 surface. Overall, the PM3 results match the density functional theory results (B3LYP/6-311+G\*\*) closely, suggesting that PM3 is a reasonable method to study this kind of reaction. This finding will allow us to investigate the enzymatic reaction directly using a hybrid PM3/MM approach. As shown from the influence of solvation effect on the reaction profile determined by a self-consistent reaction field model, there is a large reaction barrier in solution. On the basis of the above findings, the factors controlling the catalytic efficacy of the 4-chlorobenzoyl CoA dehalogenase were examined. We also studied the hydrolysis of the aryl–enzyme intermediate and a related nucleophilic aromatic substitution reaction between tetrachlorohydroquinone and glutathione (as modeled by thiomethoxide). In addition, a simple explanation concerning the previously unresolved abnormal Brønsted behavior of Tyr6Phe mutant of a  $\mu$  class glutathione S-transferase is provided.

## Introduction

Biodehalogenation by microorganisms is a cost-effective and environment-friendly alternative treatment of contamination of soil, surface, and groundwater supplies by halogenated organic compounds such as PCBs, pentachlorophenol, various herbicides, pesticides, and industrial solvents.<sup>1</sup> To facilitate bioremediation, it is important to have a fundamental understanding of the enzymes involved in these biodegradation processes. Knowledge of the catalytic mechanism and the structure–function relationship of these enzymes is a prerequisite for rational redesign of microbial enzymes for bioremediation and industrial and biotechnological purposes. Thus, dehalogenation enzymes are being intensively studied. One such enzyme is 4-chlorobenzoyl CoA dehalogenase.

The hydrolysis of 4-chlorobenzoate to 4-hydroxybenzoate is carried out by three enzymes (Scheme 1).<sup>2</sup> 4-Chlorobenzoic acid is first esterified by coenzyme A, which is catalyzed by 4-chlorobenzoyl CoA ligase. The 4-chlorobenzoyl CoA becomes the substrate for 4-chlorobenzoyl CoA dehalogenase (EC 3.8.1.6), and the product of the dehalogenation reaction (4-

## Scheme 1



hydroxybenzoyl CoA) is then converted to 4-hydroxybenzoic acid by 4-hydroxybenzoyl-CoA thioesterase. 4-Chlorobenzoyl CoA dehalogenase is particularly interesting since it is one of only a few enzymes that catalyze nucleophilic aromatic substitution reactions. It has been studied intensively by the groups of Dunaway-Mariano,<sup>3</sup> Lingens,<sup>4</sup> and Copley.<sup>5</sup> Initially, it was generally believed that the dehalogenation is a direct hydrolytic process.<sup>2,3a,5a–c</sup> This aromatic hydrolytic dehalogenase was

\* Author to whom correspondence should be addressed: tcbuice@bioorganic.ucsb.edu; (805) 893-2044 (phone); (805) 893-2229 (fax).

<sup>⊗</sup> Abstract published in *Advance ACS Abstracts*, April 15, 1997.

(1) (a) Fetzner, S.; Lingens, F. *Microbiol. Rev.* **1994**, *58*, 641. (b) Prince, R. C. *Trends Biochem. Sci.* **1994**, *19*, 3. (c) Slater, J. H.; Bull, A. T.; Hardman, D. J. *Biodegradation* **1995**, *6*, 181. (d) Wackett, L. P.; Logan, M. S. P.; Blocki, F. A.; Cai, B. *Biodegradation* **1992**, *3*, 19. (e) Janssen, D. B.; van der Plog, J. R.; Pries, F. *Environ. Health Perspect. Suppl.* **1995**, *103*, 29. (f) Leisinger, T.; Braus-Stromeier, S. A. *Environ. Health Perspect. Suppl.* **1995**, *103*, 33.

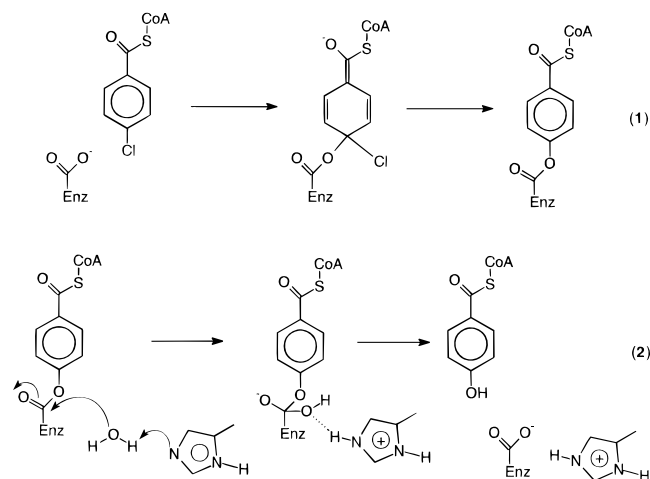
(2) Dunaway-Mariano, D.; Babbitt, P. C. *Biodegradation* **1994**, *5*, 259.

(3) (a) Scholten, J. D.; Chang, K.-H.; Babbitt, P. C.; Charest, H.; Sylvestre, M.; Dunaway-Mariano, D. *Science* **1991**, *253*, 182. (b) Liang, P.-H.; Yang, G.; Dunaway-Mariano, D. *Biochemistry* **1993**, *32*, 12245. (c) Yang, G.; Liang, P.-H.; Dunaway-Mariano, D. *Biochemistry* **1994**, *33*, 8527. (d) Taylor, K. L.; Liu, R.-Q.; Liang, P.-H.; Price, J.; Dunaway-Mariano, D.; Tonge, P. J.; Clarkson, J.; Carey, P. R. *Biochemistry* **1995**, *34*, 13881. (e) Liu, R.-Q.; Liang, P.-H.; Scholten, J.; Dunaway-Mariano, D. *J. Am. Chem. Soc.* **1995**, *117*, 5003.

(4) (a) Löffler, F.; Mueller, R.; Lingens, F. *Biochem. Biophys. Res. Commun.* **1991**, *176*, 1106. (b) Loeffler, F.; Lingens, F.; Mueller, R. *Biodegradation* **1995**, *6*, 203.

(5) (a) Copley, S. D.; Crooks, G. P. *Appl. Environ. Microbiol.* **1992**, *58*, 1385. (b) Crooks, G. P.; Copley, S. D. *J. Am. Chem. Soc.* **1993**, *115*, 6422. (c) Crooks, G. P.; Copley, S. D. *Biochemistry* **1994**, *33*, 11645. (d) Crooks, G. P.; Xu, L.; Barkley, R. M.; Copley, S. D. *J. Am. Chem. Soc.* **1995**, *117*, 10791.

## Scheme 2



believed to be mechanistically related to epoxide hydrolase and haloalkane dehalogenase that catalyze hydrolytic reactions at saturated carbon centers ( $sp^3$  carbon vs  $sp^2$  carbon in the 4-chlorobenzoyl CoA dehalogenase). Since these two enzymes were shown to follow an indirect hydrolytic process,<sup>6,7</sup> involving the formation of a covalent alkyl-enzyme intermediate, Dunaway-Mariano and co-workers<sup>3c</sup> reexamined the catalytic mechanism of 4-chlorobenzoyl CoA dehalogenase using isotope-labeled water; these results were interpreted as evidence for the formation of an aryl-enzyme covalent intermediate. This interpretation has since been confirmed by other studies.<sup>3d,e,5d</sup> According to this new mechanism, instead of a direct hydrolysis by water, the hydrolysis of 4-chlorobenzoyl CoA is initiated by the attack of a carboxylate group at the 4-position of the 4-chlorobenzoyl CoA (Scheme 2) via an  $S_NAr$  mechanism forming a covalent enzyme-phenolic ester intermediate. Subsequently, this aryl-enzyme intermediate undergoes hydrolysis by an enzyme-activated water, yielding the final product (4-hydroxybenzoyl CoA).<sup>3c-e,5d,8</sup> Recently, the X-ray crystal structure of 4-chlorobenzoyl CoA dehalogenase with bound product (4-hydroxybenzoyl CoA) has been solved at 1.8 Å resolution.<sup>9</sup> On the basis of these crystallographic<sup>9</sup> and mutagenesis studies,<sup>10</sup> the carboxylate of Asp145 is identified to be the attacking nucleophile and His90 to be the base that activates water during the subsequent hydrolysis of the covalent aryl-enzyme intermediate. However, interestingly, the X-ray structure does not show the presence of this water in the crystal structure of the enzyme with bound 4-hydroxybenzoyl CoA.

Aromatic nucleophilic substitution reactions are usually believed to follow a two-step process.<sup>11,12</sup> The first step involves the addition of nucleophile to the aromatic ring, forming a Meisenheimer intermediate (or  $\sigma$ -complex). In the second step,

(6) Verschueren, K. H. G.; Seljee, F.; Rozeboom, H. J.; Kalk, K. H.; Dijkstra, B. W. *Nature* **1993**, *363*, 693.

(7) Lacourciere, G. M.; Armstrong, R. N. *J. Am. Chem. Soc.* **1993**, *115*, 10466. Lacourciere, G. M.; Armstrong, R. N. *Chem. Res. Toxicol.* **1994**, *7*, 122.

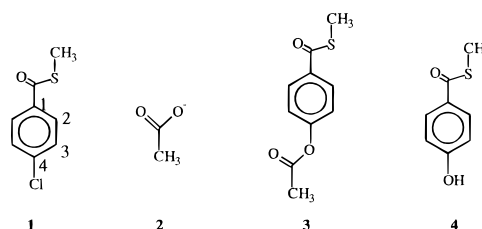
(8) Zheng, Y.-J.; Ornstein, R. L. *Protein Eng.* **1996**, *9*, 231.

(9) Benning, M. M.; Taylor, K. L.; Liu, R.-Q.; Yang, G.; Xiang, H.; Wesenberg, G.; Dunaway-Mariano, D.; Holden, H. M. *Biochemistry* **1996**, *35*, 8103.

(10) (a) Yang, G.; Liu, R.-Q.; Taylor, K. L.; Xiang, H.; Price, J.; Dunaway-Mariano, D. *Biochemistry* **1996**, *35*, 10879. (b) Taylor, K. L.; Xiang, H.; Liu, R.-Q.; Yang, G.; Dunaway-Mariano, D. *Biochemistry* **1997**, *36*, 1349.

(11) (a) Bunnett, J. F.; Zahler, R. E. *Chem. Rev.* **1951**, *49*, 340. Bunnett, J. F.; Davis, G. T. *J. Am. Chem. Soc.* **1954**, *76*, 3011. Bunnett, J. F.; Snipes, R. F. *J. Am. Chem. Soc.* **1955**, *77*, 5422. Bunnett, J. F.; Garbisch, E. W., Jr.; Pruitt, K. M. *J. Am. Chem. Soc.* **1957**, *79*, 385. Bunnett, J. F.; Merritt, W. D., Jr. *J. Am. Chem. Soc.* **1957**, *79*, 5967. (b) Miller, J. *Aromatic Nucleophilic Substitution*; Elsevier: Amsterdam, The Netherlands, 1968.

## Scheme 3



the Meisenheimer intermediate undergoes leaving group (e.g.,  $Cl^-$ ) expulsion and yields the product. The formation of the Meisenheimer intermediate is the rate-determining step for many nucleophilic aromatic substitution reactions. In some special cases, the Meisenheimer intermediate has been isolated and characterized. The availability of a high-resolution crystal structure<sup>9</sup> of 4-chlorobenzoyl CoA dehalogenase with bound 4-hydroxybenzoyl CoA has provided a structural framework to examine the catalytic reaction mechanism and the origins of the catalytic power of this enzyme. However, to gain a deeper understanding about the enzyme catalysis, information about the simple carboxylate-catalyzed reaction is required. To the best of our knowledge, no such studies related to the uncatalyzed reaction have been reported. Furthermore, it is unlikely that this uncatalyzed reaction can be studied directly in aqueous solution for the following two reasons. First, the thioester group is more susceptible to nucleophilic attack because the thioester group is more reactive than the aromatic ring. Second, in  $S_NAr$  reactions in solution, acetate normally acts like a general base rather than a nucleophile. A recent study<sup>13</sup> has demonstrated that quantum mechanics calculations in combination with self-consistent reaction field solvent models are capable of providing valuable information regarding the nucleophilic aromatic substitution reaction in both gas phase and in solution. Here, we report a detailed theoretical investigation of the uncatalyzed dehalogenation of 4-chlorobenzoyl CoA using appropriate model compounds. Possible factors that modulate the catalytic power of 4-chlorobenzoyl CoA dehalogenase are also examined.

## Theoretical Procedure

**Ab Initio Quantum Mechanics.** All ab initio molecular orbital calculations were carried out using the *Gaussian 94* program.<sup>14</sup> Geometry optimizations were performed at the HF/6-31G\* level of theory, which has been shown to give similar geometries and energetics as the HF/6-31+G\*\* level of theory for the  $S_NAr$  reaction between 1-chloro-2,4-dinitrobenzene (CDNB) and thiomethoxide ( $CH_3S^-$ ).<sup>13</sup> Scheme 3 shows the model compounds used in this study. Geometries of each species involved were fully optimized and characterized by calculating harmonic vibrational frequencies. Transition states were characterized by the presence of one negative force constant that corresponds to the interconversion of the reactant and the product. To include electron correlation effect, further energy calculations were

(12) (a) Terrier, F. In *Nucleophilic Aromatic Displacement: The Influence of the Nitro Group*; Fever, H., Ed.; Organic Nitro Chemistry Series; VCH Publishers, Inc.: New York, 1991. (b) Chupakhin, O. N.; Charushin, V. N.; van der Plas, H. C. *Nucleophilic Aromatic Substitution of Hydrogen*; Academic Press: San Diego, CA, 1994.

(13) Zheng, Y.-J.; Ornstein, R. L. *J. Am. Chem. Soc.* **1997**, *119*, 648.

(14) *Gaussian 94*, Revision B.2; Frisch, M. J.; Trucks, G. W.; Schlegel, H. B.; Gill, P. M. W.; Johnson, B. G.; Robb, M. A.; Cheeseman, J. R.; Keith, T.; Petersson, G. A.; Montgomery, J. A.; Raghavachari, K.; Al-Laham, M. A.; Zakrzewski, V. G.; Ortiz, J. V.; Foresman, J. B.; Cioslowski, J.; Stefanov, B. B.; Nanayakkara, A.; Challacombe, M.; Peng, C. Y.; Ayala, P. Y.; Chen, W.; Wong, M. W.; Andres, J. L.; Replogle, E. S.; Gomperts, R.; Martin, R. L.; Fox, D. J.; Binkley, J. S.; Defrees, D. J.; Baker, J.; Stewart, J. P.; Head-Gordon, M.; Gonzalez, C.; Pople, J. A.; Gaussian, Inc.: Pittsburgh, PA, 1995.

carried out using the density functional theory method with Becke3LYP functionals<sup>15</sup> using 6-311+G\*\* basis set (designated as B3LYP/6-311+G\*\*).

The gas phase free energy surface was also mapped out at the B3LYP/6-311+G\*\* level of theory using the vibrational frequency calculated at the HF/6-31G\* level of theory. The thermochemical analysis was carried out at 298.15 K and 1 atm of pressure. Enthalpies were determined using the following formula<sup>16</sup>

$$\Delta H_{\text{cal}}^{298.15} = \Delta E_e^0 + \Delta E_v^0 + \Delta(\Delta E_v)^{298.15} + \Delta E_T^{298.15} + \Delta E_i^{298.15} + \Delta PV$$

where the first term is the computed electronic energy difference, while the second term is the change in zero-point vibrational energy. The third term is the change in vibrational energy on going from 0 to 298.15 K. The fourth, fifth, and the sixth terms are due to changes in rotation and translation energies, and pressure-volume work, respectively. Entropies were evaluated using a standard statistical mechanical approach;<sup>16</sup> translational, rotational, and vibrational contributions were included.

**Semiempirical Quantum Mechanics.** Semiempirical molecular orbital calculations were carried out using the AMPAC 5.0 program<sup>17</sup> using the PM3<sup>18</sup> method. We chose PM3 method for two reasons. First, PM3 is better in dealing with hydrogen bonding than AM1;<sup>19</sup> AM1 tends to give bifurcated hydrogen bonds.<sup>20</sup> Second, it is well-known that AM1 cannot treat chloride ion very well. The large error associated with chloride ion will distort the potential energy surface and make the calculated results unrealistic. On the other hand, PM3 is much better in dealing with chloride anion.<sup>18,21</sup> For solvation calculations, AMSOL (as implemented in AMPAC 5.0) was used. The reaction profile in solution was calculated using the PM3-SM3 method developed by Cramer and Truhlar.<sup>22</sup>

Since ab initio molecular orbital calculations for the S<sub>N</sub>Ar reaction between 1-chloro-2,4-dinitrobenzene and thiomethoxide have been reported,<sup>13</sup> we also checked the performance of PM3 on the same reaction. Overall, the PM3 results are very similar to the ab initio results at the HF level of theory (data not shown). The only significant difference is that the Meisenheimer intermediate is more stable on the PM3 potential energy surface. One of our goals is to be able to examine the enzymatic reaction directly in the future using a hybrid quantum mechanics and molecular mechanics (QM/MM) approach.<sup>23–25</sup> Due to the large size of the substrate, the use of high-level ab initio quantum mechanics (or density functional theory) as the QM part in the QM/MM approach would be prohibitive. On the other hand, QM/MM calculations that use semiempirical molecular orbital methods as the QM part are computationally very attractive and have been applied to several enzymes.<sup>26–28</sup> Although semiempirical molecular orbital methods are fast, they are generally less reliable than high-level ab initio or density functional theory methods. Thus, before applying semiempirical methods to enzymatic reactions, it is important to

(15) (a) Becke, A. D. *J. Chem. Phys.* **1993**, *98*, 5648. (b) Lee, C.; Yang, W.; Parr, R. G. *Phys. Rev. B* **1988**, *37*, 785.

(16) Hehre, W. J.; Radom, L.; Schleyer, P. v. R.; Pople, J. A. *Ab Initio Molecular Orbital Theory*; Wiley-Interscience: New York, 1986.

(17) AMPAC 5.0, 1994; Semichem, 7128 Summit, Shawnee, KS 66216.

(18) Stewart, J. J. P. *J. Comput. Chem.* **1989**, *10*, 209, 221. Stewart, J. J. P. *J. Comput. Chem.* **1991**, *12*, 320.

(19) Dewar, M. J. S.; Zoebisch, E. G.; Healy, E. F.; Stewart, J. J. P. *J. Am. Chem. Soc.* **1985**, *107*, 3902.

(20) Zheng, Y.-J.; Merz, K. M., Jr. *J. Comput. Chem.* **1992**, *13*, 1151.

(21) Hartsough, D. S.; Merz, K. M., Jr. *J. Phys. Chem.* **1995**, *99*, 384.

(22) Cramer, C. J.; Truhlar, D. G. *J. Comput.-Aided Mol. Des.* **1992**, *6*, 629.

(23) Warshel, A.; Levitt, M. *J. Mol. Biol.* **1976**, *103*, 227. Luzhkov, V.; Warshel, A. *J. Comput. Chem.* **1992**, *13*, 199.

(24) Field, M. J.; Bash, P. A.; Karplus, M. *J. Comput. Chem.* **1990**, *11*, 700.

(25) Singh, U. C.; Kollman, P. A. *J. Comput. Chem.* **1986**, *7*, 718.

(26) Bash, P. A.; Field, M. J.; Davenport, R. C.; Petsko, G. A.; Ringe, D.; Karplus, M. *Biochemistry* **1991**, *30*, 5826.

(27) Lyne, P. D.; Mulholland, A. J.; Richards, W. G. *J. Am. Chem. Soc.* **1995**, *117*, 11345.

(28) Hartsough, D.; Merz, K. M., Jr. *J. Phys. Chem.* **1995**, *99*, 11266. Merz, K. M., Jr.; Banci, L. *J. Phys. Chem.* **1996**, *100*, 17414.

**Table 1.** The Calculated Electronic Energy (au, 1 au = 627.5 kcal/mol) for Each Species Involved in This Study

| compound              | HF/6-31G*     | B3LYP/6-311+G** |
|-----------------------|---------------|-----------------|
| <b>1</b>              | -1238.8880085 | -1242.8452713   |
| acetate               | -227.225068   | -228.600829     |
| <b>RC1</b>            | -1466.1382538 | -1471.4669613   |
| <b>RC2</b>            | -1466.1423363 | -1471.4709593   |
| <b>TS</b>             | -1466.090859  | -1471.4382729   |
| <b>PC</b>             | -1466.1827788 | -1471.493034    |
| <b>P</b>              | -1006.6325415 | -1011.1657169   |
| <b>Cl<sup>-</sup></b> | -459.525997   | -460.3037272    |

**Table 2.** The Calculated Thermal Energy (kcal/mol) and Entropy (cal/(mol K)) for Each Species Involved in This Study at the HF/6-31G\* Level

| compound              | thermal energy | entropy |
|-----------------------|----------------|---------|
| <b>1</b>              | 94.072         | 103.139 |
| acetate               | 35.421         | 69.698  |
| <b>RC2</b>            | 131.444        | 141.628 |
| <b>TS</b>             | 130.093        | 128.085 |
| <b>PC</b>             | 132.489        | 133.727 |
| <b>P</b>              | 130.785        | 121.492 |
| <b>Cl<sup>-</sup></b> | 0.889          | 36.586  |

calibrate against either experimental data or results from high-level ab initio calculations. By comparing the performance of ab initio and semiempirical quantum mechanical results for the reaction in the gas phase, one could evaluate the accuracy and the suitability of employing semiempirical quantum mechanics method in the study of a particular enzymatic reaction.

The hydrolysis of the aryl-enzyme intermediate by a His90-activated water molecule was also examined with the PM3 method.

## Results and Discussion

Dehalogenation via an enzyme-catalyzed nucleophilic substitution is of considerable interest. Among the well-known dehalogenation enzymes are haloalkane dehalogenase,<sup>6a</sup> haloacid dehalogenase,<sup>29</sup> 4-chlorobenzoyl CoA dehalogenase,<sup>2</sup> and tetrachlorohydroquinone dehalogenase.<sup>30</sup> To gain a better understanding of how 4-chlorobenzoyl CoA dehalogenase functions, we hereby examine the reaction of AcO<sup>-</sup> with a thioester of 4-chlorobenzoic acid (model for 4-chlorobenzoyl CoA). The nucleophilic aromatic substitution reaction between 4-Cl-Ph-CO-SCH<sub>3</sub> and CH<sub>3</sub>COO<sup>-</sup> was first investigated in the gas phase using both ab initio and semiempirical molecular orbital theory methods. Tables 1–3 summarize the calculated total electronic energy, thermal energy and entropy, and heat of formation for each species involved in this reaction, respectively.

**Gas Phase Reaction.** So far, only a few gas phase nucleophilic aromatic substitution reactions have been investigated either experimentally<sup>31</sup> or theoretically.<sup>13,32</sup> Study of gas phase nucleophilic reactions are often complicated by competing

(29) Soda, K.; Kurihara, T.; Liu, J.-Q.; Nardi-Dei, V.; Park, C.; Miyagi, M.; Tsunasawa, S.; Esaki, N. *Pure Appl. Chem.* **1996**, *68*, 2097. Hisano, T.; Hata, Y.; Fujii, T.; Liu, J.-Q.; Hurihara, T.; Esaki, N.; Soda, K. *J. Biol. Chem.* **1996**, *271*, 20322.

(30) (a) Xun, L.; Topp, E.; Orser, C. S. *J. Bacteriol.* **1992**, *174*, 8003. (b) Xun, L.; Topp, E.; Orser, C. S. *Biochem. Biophys. Res. Commun.* **1992**, *182*, 361. (c) Orser, C. S.; Dutton, J.; Lange, C.; Jablonski, P.; Xun, L.; Hargis, M. *J. Bacteriol.* **1993**, *175*, 2640. (d) McCarthy, D. L.; Navarrete, S.; Willett, W. S.; Babbitt, P. C.; Copley, S. D. *Biochemistry* **1996**, *35*, 14634. (e) Willett, W. S.; Copley, S. D. *Chem. Biol.* **1996**, *3*, 851.

(31) (a) Ingemann, S.; Nibbering, N. M. M.; Sullivan, S. A.; DePuy, C. H. *J. Am. Chem. Soc.* **1982**, *104*, 6520. (b) Ingemann, S.; Nibbering, N. M. M. *J. Org. Chem.* **1983**, *48*, 183. (c) Ingemann, S.; Nibbering, N. M. M. *N. J. Chim.* **1984**, *8*, 299.

(32) (a) Simkin, B. Y.; Gluz, E. B.; Glukhovtsev, M. N.; Minkin, V. I. *J. Mol. Struct. (THEOCHEM)* **1993**, *284*, 123. (b) Dotterer, S. K.; Harris, R. L. *J. Org. Chem.* **1988**, *53*, 777. (c) Bacaloglu, R.; Bunton, C. A.; Ortega, F. *J. Am. Chem. Soc.* **1989**, *111*, 1041.

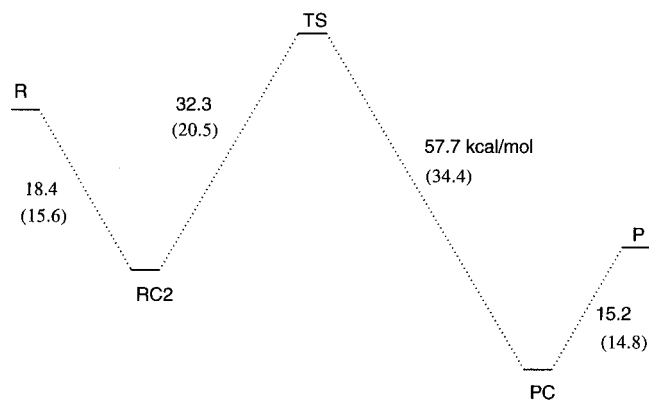
**Table 3.** The Calculated Heat of Formation (kcal/mol) and Solvation Free Energy (kcal/mol) for Each Species Involved in This Study Using PM3 and PM3-SM3 Methods, Respectively

| compound              | $\Delta H_f$ | $\Delta H_f + \text{solvation free energy}$ |
|-----------------------|--------------|---------------------------------------------|
| <b>1</b>              | -13.43       | -21.2                                       |
| acetate               | -119.65      | -194.1                                      |
| <b>RC1</b>            | -147.49      | -212.1                                      |
| <b>RC2</b>            | -146.84      | -204.1                                      |
| <b>TS1</b>            | -128.60      | -187.9                                      |
| <b>INT</b>            | -144.25      | -204.0                                      |
| <b>TS2</b>            | -144.19      | -205.0                                      |
| <b>PC</b>             | -162.46      | -225.8                                      |
| <b>P</b>              | -86.83       | -97.1                                       |
| <b>Cl<sup>-</sup></b> | -51.23       | -128.2                                      |

reactions such as proton transfer and  $S_N2$  reactions. The Fourier transform ion cyclotron resonance study on the gas phase reactions of pentafluorophenyl ethers with several different nucleophiles seems to indicate the presence of the loosely bound ion–molecule complexes which have a long enough lifetime to allow secondary reactions to take place.<sup>31a</sup> However, it is not clear from these studies whether the Meisenheimer complex is a minimum or a maximum (transition state) on the potential energy surface. The presence of loosely bound ion–molecule and Meisenheimer intermediate ( $\sigma$ -complex) in the gas phase has also been demonstrated for systems such as  $\text{Cl}^-(\text{C}_6\text{H}_6)$ ,  $\text{F}^-(\text{C}_6\text{H}_6)$ , and  $\text{F}^-(\text{C}_6\text{F}_6)$ .<sup>33</sup> Recently, ab initio molecular orbital theory was used to elucidate the nucleophilic aromatic reaction between 1-chloro-2,4-dinitrobenzene (CDNB) and thiomethoxide in gas phase and in solution.<sup>13</sup> It was found that the overall gas phase reaction profile has three potential wells (minima). The first one corresponds to the reactant-side ion–molecule complex, the second one the Meisenheimer intermediate, and the third one the product-side ion–molecule complex. However, in solution, the two ion–molecule complexes are not minima on the potential energy surface; only the Meisenheimer intermediate still exists as a minimum. The formation of the Meisenheimer intermediate was calculated to be the rate-determining step, which is in good agreement with experimental observation; the calculated reaction free energy barrier in solution also seems to be in good agreement with experimental data.

To elucidate the reaction between 4-Cl-Ph-CO-SCH<sub>3</sub> and CH<sub>3</sub>COO<sup>-</sup>, first, the geometries of the reactants, ion–molecule complexes, and the products were optimized at the HF/6-31G\* level of theory. The transition state was located and characterized by calculating the harmonic vibrational frequencies. The calculated potential energy profile and the optimized geometries at the HF/6-31G\* level of theory are shown in Figures 1 and 2, respectively. The overall reaction profile is similar to what was observed for the reaction between CDNB and thiomethoxide with the exception that no minimum corresponding to the Meisenheimer intermediate was located in the current system. In the previous ab initio molecular orbital study on the reaction of CDNB with thiomethoxide, a very shallow minimum corresponding to the Meisenheimer intermediate was located at both HF/6-31G\* and HF/6-31+G\*\* levels of theory. This sensibly indicates that nitro groups are more effective in stabilizing the negative charge in the Meisenheimer intermediate than the -CO-SCH<sub>3</sub> group.

The gas phase reaction between 4-Cl-Ph-CO-SCH<sub>3</sub> and CH<sub>3</sub>COO<sup>-</sup> seems to be concerted. The overall reaction barrier is about 4.9 kcal/mol at the B3LYP/6-311+G\*\* level of theory; the barrier from the ion–molecule complex is about 32.3 kcal/mol. The overall reaction is exothermic by 14.6 kcal/mol. It is

**Figure 1.** The calculated potential energy surface for the nucleophilic aromatic reaction between 4-Cl-Ph-CO-SCH<sub>3</sub> and CH<sub>3</sub>COO<sup>-</sup> in the gas phase at the HF/6-31G\* and B3LYP/6-311+G\*\* (in parentheses) levels of theory. RC2 refers to the most stable reactant-side ion–molecule complex.

not clear presently if at a higher level of theory the Meisenheimer intermediate exists as a minimum on the potential energy surface. Since both reactant-side and product-side ion–molecule complexes are relatively stable, they may have a long enough lifetime in the gas phase to allow direct experimental investigations. However, it should be noted that side reactions may complicate such a study. For instance, the thioester may be susceptible to attack by carboxylate, which is not a problem for the enzymatic reaction since the enzyme restricts the position of the nucleophile (carboxylate) such that it is geometrically impossible for such a side reaction to take place.

4-Cl-Ph-CO-SCH<sub>3</sub> adapts a planar structure as seen in the X-ray structure of 4-chlorobenzoyl CoA dehalogenase with bound 4-hydroxybenzoyl CoA. The ion–molecule complex formed between 4-Cl-Ph-CO-SCH<sub>3</sub> and CH<sub>3</sub>COO<sup>-</sup> is also planar. Since the four hydrogens of the aromatic ring are not equivalent, two ion–molecule complexes (**RC1** and **RC2**) can form. The energy difference between these two ion–molecule complexes are relatively small, the calculated energy difference being 2.6 and 2.5 kcal/mol at HF/6-31G\* and B3LYP/6-311+G\*\* levels of theory, respectively. The carboxylate oxygen atoms form weak C–H···O hydrogen bonds with two of the four aromatic hydrogens. The H···O distances are about 2.12 and 2.30 Å in compound **RC1**, and 2.15 and 2.17 Å in **RC2**, respectively. In the transition state, the C···O distance is about 1.85 Å and the C–Cl bond is about 1.79 Å. The carbon atom is slightly pyramidal, and the C–Cl bond lengthens by about 0.05 Å (1.79 Å in **TS** vs 1.74 Å in **1**). In the product-side ion–molecule complex, the leaving chloride ion is hydrogen bonded to one of the methyl hydrogens of the acetate moiety (Cl<sup>-</sup>···H distance being 2.7 Å) and one of the aromatic hydrogens (2.64 Å). The ester moiety of the product-side ion–molecule complex is twisted out of plane to allow the weak C–H···O interaction. In the product, the thioester moiety is coplanar with the aromatic ring, but the ester group is twisted out of the aromatic ring plane by about 58°.

Figure 3 shows the calculated free energy surface in gas phase at the B3LYP/6-311+G\*\* level of theory. Formation of both ion–molecule complexes from corresponding isolated components are entropically unfavorable, therefore, the minima become shallower on the free energy surface; the calculated free energies of formation for these two ion–molecule complexes are 4.9 and 7.3 kcal/mol, respectively (see Figure 3). The reaction has an overall free energy barrier of 18.3 kcal/mol, and the free energy of reaction is 8.1 kcal/mol.

The calculated PM3 potential energy surface and optimized geometries are shown in Figures 4 and 5, respectively. Overall,

(33) Hiraoka, K.; Mizuse, S.; Yamabe, S. *J. Chem. Phys.* **1987**, *86*, 4102.

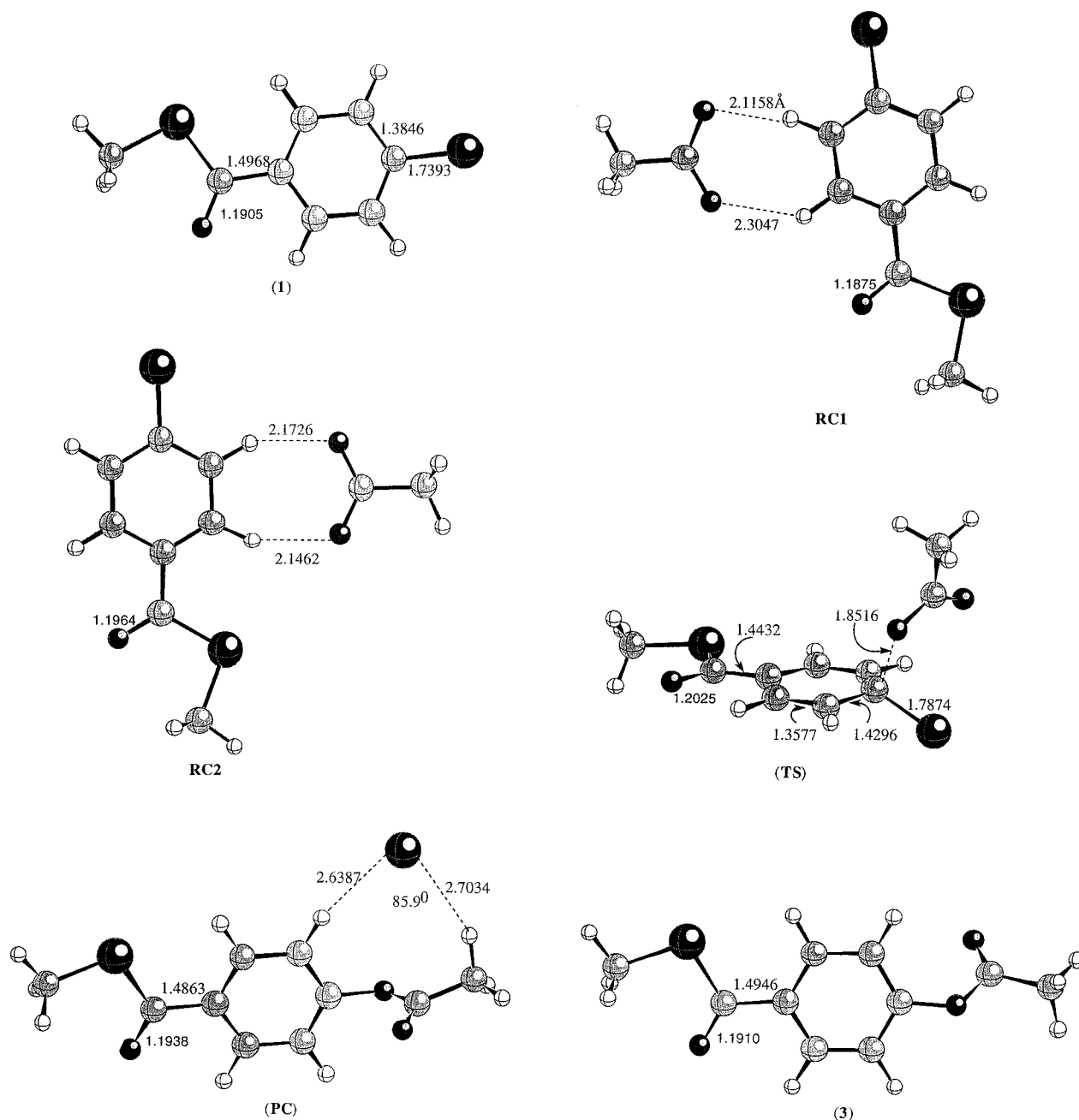


**Figure 2.** The optimized geometries for species involved at HF/6-31G\* level of theory.

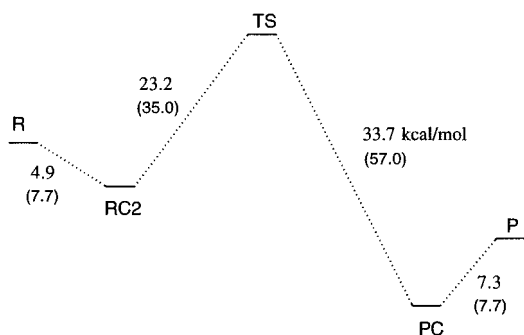


**Figure 3.** The calculated free energy surface for the nucleophilic aromatic reaction between 4-Cl-Ph-CO-SCH<sub>3</sub> and CH<sub>3</sub>COO<sup>-</sup> in the gas phase at the B3LYP/6-311+G\*\* level of theory. The HF/6-31G\* values are in parentheses.

the potential energy surface resembles the B3LYP/6-311+G\*\* surface closely. However, a very shallow minimum corresponding to the Meisenheimer intermediate was located on the

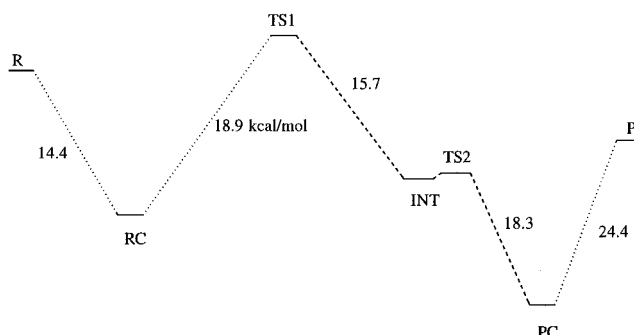


**Figure 4.** The calculated potential energy surface with PM3 method.

PM3 surface; the transition state for the Cl<sup>-</sup> expulsion is only slightly higher in energy than the Meisenheimer intermediate. It is possible that in solution or in the active site of dehalogenase the Meisenheimer complex could be much more stable than in the gas phase. Again, the reaction is predicted to be exothermic

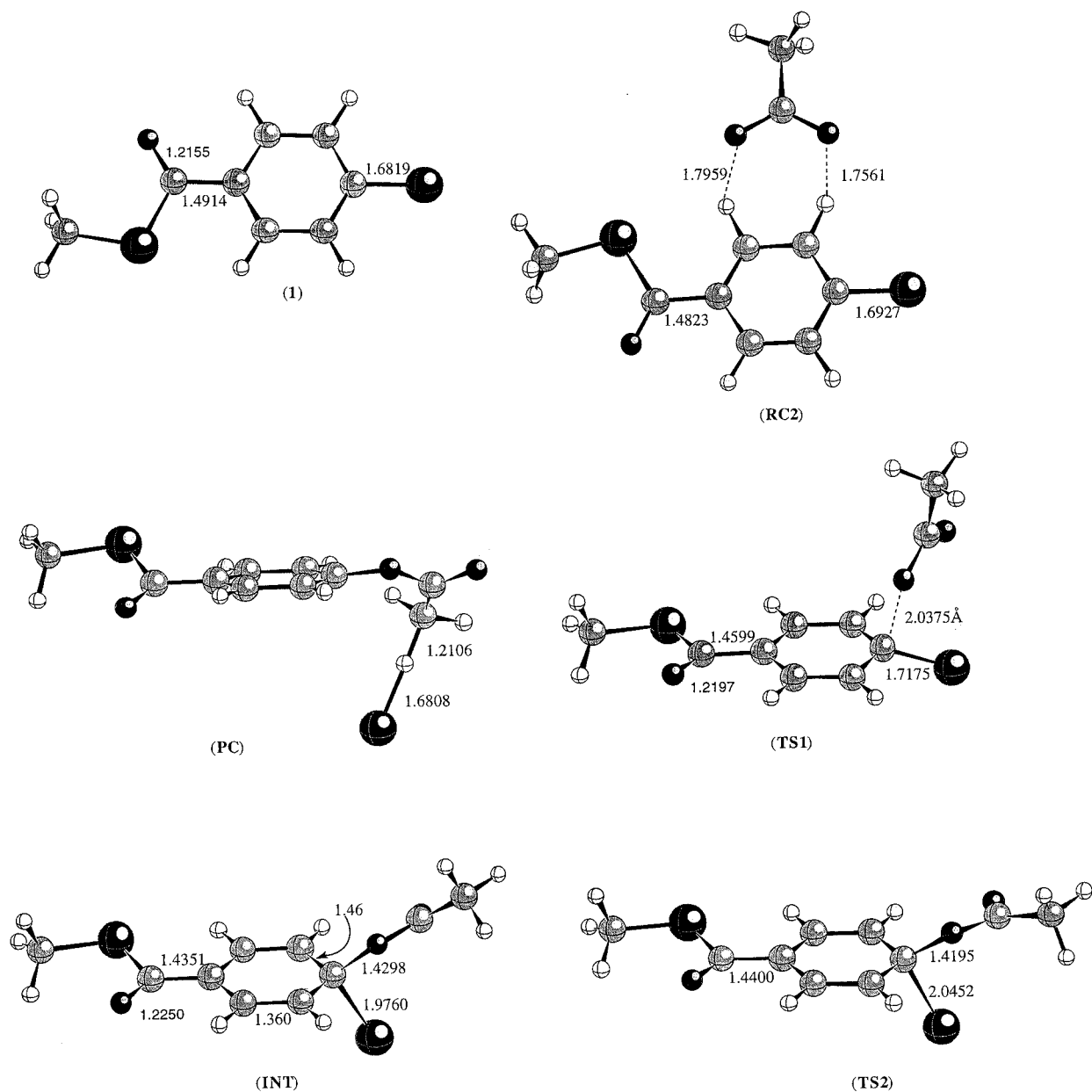


Figure 5. The PM3-optimized geometries.

in the gas phase. The transition state on the HF/6-31G\* surface corresponds to the first transition state on the PM3 surface.

The optimized geometries with PM3 are in general very similar to the optimized ab initio geometries. The transition state is also very similar to the HF/6-31G\* transition state. In the PM3 calculated transition state (the first transition state), the C $\cdots$ O distance is about 2.04 Å and the C-Cl bond is about 1.72 Å, with the C $\cdots$ O distance being about 0.19 Å longer than the HF/6-31G\* results. As expected, the six-membered ring of the Meisenheimer intermediate is still planar. The C-Cl and C<sub>4</sub>-O distances are about 1.98 and 1.43 Å, respectively, which are longer than normal covalent bonds. The C<sub>1</sub>-C(=O) distance becomes about 0.07 Å shorter in the Meisenheimer intermediate compared to the same bond in the reactant, indicating charge delocalization from the six-membered ring to the thioester carbonyl moiety. This charge delocalization would further be enhanced by the presence of hydrogen bond donor groups near the carbonyl oxygen of the thioester group. In the second transition state for the breaking of the C-Cl bond, the C-Cl distance is about 2.05 Å and the C<sub>4</sub>-O distance is about 1.42 Å. For the product **4**, several conformations exist

depending on the orientation of the thioester and ester moiety relative to the aromatic ring. The planar conformation with both the thioester and ester groups coplanar to the aromatic ring is about 2.3 kcal/mol higher in energy than the one with both groups twisted out of the plane of the aromatic ring. It is well-known that semiempirical molecular orbital methods tend to underestimate the rotational barriers.<sup>19</sup> The PM3-optimized product-side ion-molecule complex is different from the ab initio one in that there is only weak Cl<sup>-</sup> $\cdots$ H-C hydrogen bond in the PM3 structure.

**Aqueous Solution.** Solvation has a great impact on nucleophilic substitution reactions that involve ionic species.<sup>34</sup> For example, the S<sub>N</sub>Ar reaction between *p*-nitrofluorobenzene and N<sub>3</sub><sup>-</sup> is about 12 000 times faster in dipolar aprotic solvents such as dimethylsulfoxide.<sup>34a</sup> Small anions are much better solvated in protic solvents such as methanol and water, which makes them less reactive. To estimate the reaction barrier in aqueous solution, we calculated the reaction profile in solution using the method developed by Cramer and Truhlar.<sup>22</sup> In these

(34) (a) Parker, A. J. *Q. Rev. Chem. Soc.* **1962**, *16*, 163. (b) Jorgensen, W. L. *Acc. Chem. Res.* **1989**, *22*, 184.

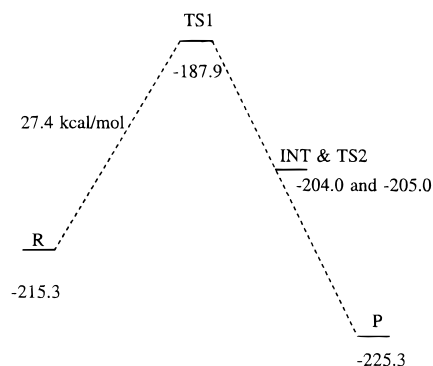


**Figure 6.** The calculated reaction profile in solution using the PM3-SM3 method.

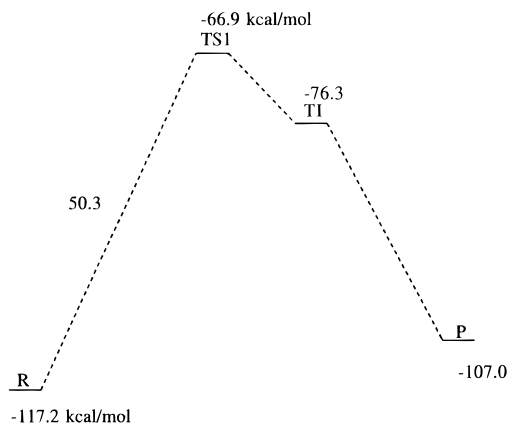


**Figure 7.** The calculated potential energy surface for the hydrolysis of the ester intermediate using PM3 semiempirical molecular orbital method.

solvation calculations, the gas phase geometries were used without relaxation.<sup>35</sup> Since geometry optimization and transition state search in solution are very time consuming, gas phase geometries are generally used in solvation calculations, and this has been shown to be a valid approach.<sup>35</sup> The calculated energy, which is a combination of the heat of formation and solvation free energy, for each species is given in Table 3. As seen from Table 3, the two ion–molecule complexes in solution are no longer minima. There is a large barrier for this nucleophilic aromatic substitution reaction in solution (Figure 6). The estimated barrier is about 27.4 kcal/mol, which does not include entropy contribution. When the entropic contribution is made, on the basis of PM3-calculated harmonic vibrational frequencies, the free energy barrier is estimated to be about 37.4 kcal/mol. Clearly, this reaction would be very slow in aqueous solution.

**Hydrolysis of the Aryl–Enzyme Intermediate.** PM3 calculations were also carried out to examine the hydrolysis of the aryl–enzyme intermediate. Active site His90 was modeled using imidazole, and the aryl–enzyme intermediate is modeled by **4** (see Scheme 3). The calculated reaction profile in gas phase is shown in Figure 7, and the optimized geometries are shown in Figure 8. The hydrolysis step is related to reactions catalyzed by haloalkane dehalogenase,<sup>6a</sup> serine proteases, lipases, and esterases.<sup>36,37</sup> These enzymes normally employ a catalytic Asp(Glu)–His–Ser triads; in one case, it was found that the orientation of the His can be controlled by a neutral hydrogen bond donor.<sup>37</sup> A similar mechanism for the 4-chlorobenzoyl

CoA dehalogenase catalyzed hydrolysis of the aryl–enzyme ester intermediate is as follow. The hydrolysis is initiated by the attack of a water molecule that is activated by His90 in the active site of the enzyme on the aryl–enzyme ester to form a tetrahedral intermediate; then, the breaking down of the tetrahedral intermediate follows. This proposed mechanism involves a charge separation; therefore, in the gas phase, the model reaction has a very high barrier. According to the PM3 calculations on a model system, the initial barrier is about 50.3 kcal/mol, which is probably overestimated since the semiempirical method tends to overestimate proton transfer barriers.<sup>38</sup> The tetrahedral intermediate is only of marginal stability. In fact, we could not find the transition state for the breaking down of the tetrahedral intermediate. In the enzymatic reaction, the negative charge on the oxygen atom (oxyanion) in the intermediate is stabilized by active site residues (e.g., Trp137) through hydrogen-bonding interactions as seen in serine proteases. The reaction barrier would be much smaller for the enzymatic reaction. As shown in Figure 8, the proton transfer from water to imidazole is not yet complete in the transition state, indicating that the proton transfer and the nucleophilic attack at the ester carbon occur not as separated steps, but instead occur in a concerted fashion, which is consistent with the mechanistic proposals concerning related enzymes such as serine proteases.<sup>36</sup>

**Enzymatic Reaction.** Since we now have a detailed understanding of the uncatalyzed reaction both in the gas phase and in solution, it may be worthwhile examining the possible factors that contribute to the catalytic power of 4-chlorobenzoyl CoA dehalogenase. As demonstrated above, the gas phase reaction is relatively fast and requires little activation energy; however, the solution reaction is very slow due to the large solvation effect. Obviously, the enzyme could accelerate this reaction by providing a nonaqueous environment where the reaction could take place without much interference from solvent molecules.

The active site environment, as recently revealed by the X-ray crystallographic study of Holden,<sup>9</sup> is depicted in Scheme 4 where the pseudosubstrate is 4-hydroxybenzoyl CoA. As shown, the side chain carboxylate of Asp145 is held above the benzoyl ring of 4-hydroxybenzoyl CoA via hydrogen bonding by the Trp137. The distance between the attacking oxygen of the carboxylate and the C<sub>4</sub> is about 2.89 Å in the X-ray crystal structure, which would be even smaller in the complex of dehalogenase with bound 4-chlorobenzoyl CoA since the hydrogen-bonding interaction between the attacking oxygen and the 4-HO would be absent for a 4-Cl substituent. Clearly, the enzyme is capable of orienting the carboxylate to such a position that nucleophilic aromatic substitution could occur with little geometrical rearrangement. The formation of the ion–molecule complex in the gas phase reaction (*loc. cit.*) is probably counterproductive since the nucleophile lies in the plane of the benzoyl ring, while for nucleophilic aromatic substitution to take place, the nucleophile has to be placed above the plane. The enzyme solves this problem by directly placing the nucleophile (the carboxylate of Asp145) in the right orientation relative to the benzoyl ring. This is reminiscent of the recently proposed “near attack conformation” (NAC) concept.<sup>39</sup>

The dehalogenase apparently orients the substrate and the nucleophile in such a fashion to form a NAC. Recent studies have demonstrated that Trp137 is not essential for substrate binding; however, it is very important for catalysis.<sup>10</sup> When

(35) Tomasi, J.; Persico, M. *Chem. Rev.* **1994**, *94*, 2027.

(36) Steitz, T. A.; Schulman, R. G. *Ann. Rev. Biophys. Bioeng.* **1982**, *11*, 419.

(37) (a) Schrag, J. D.; Li, Y.; Wu, S.; Cygler, M. *Nature* **1991**, *351*, 761. (b) Wei, Y.; Schottel, J. L.; Derewenda, U.; Swenson, L.; Patkar, S.; Derewenda, Z. S. *Nat. Struct. Biol.* **1995**, *2*, 218.

(38) Zheng, Y.-J.; Merz, K. M., Jr.; Farber, G. K. *Protein Eng.* **1993**, *6*, 479.

(39) Lightstone, F. C.; Bruice, T. C. *J. Am. Chem. Soc.* **1996**, *118*, 2595.

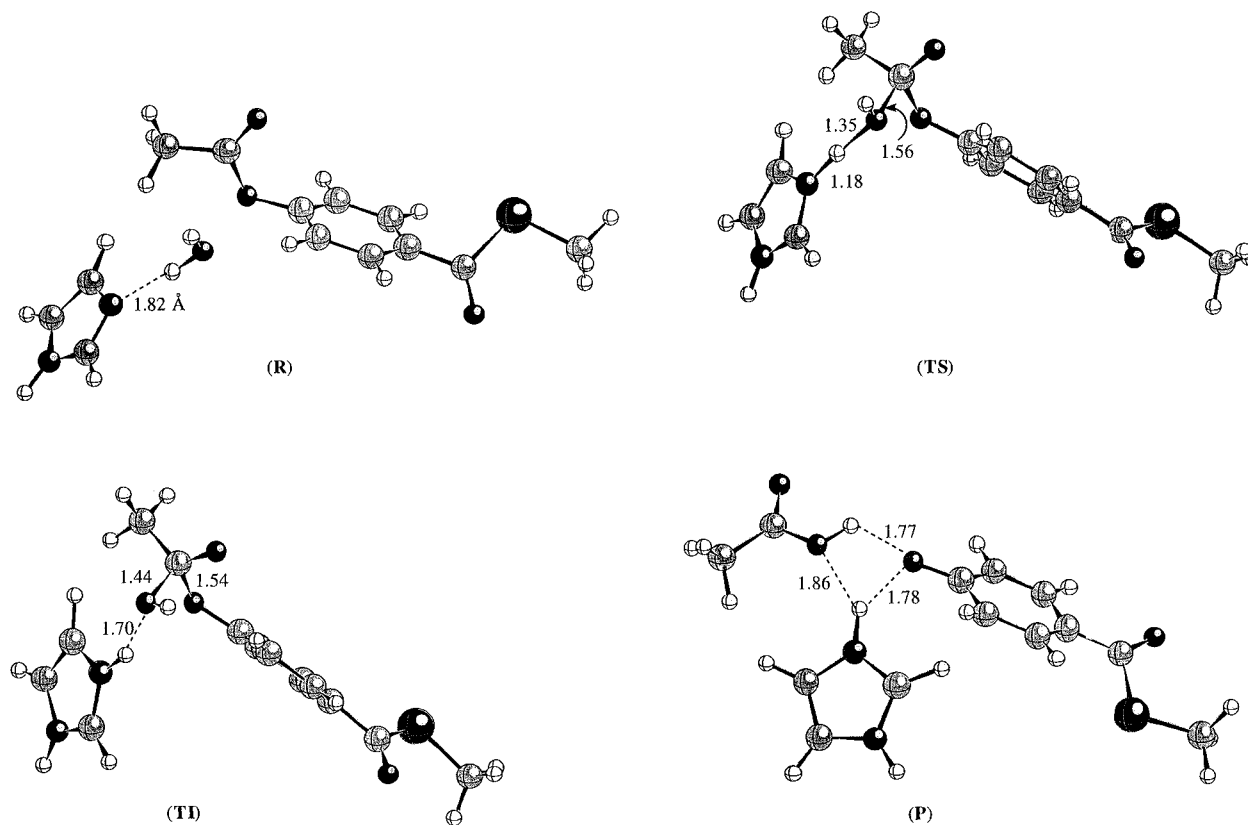
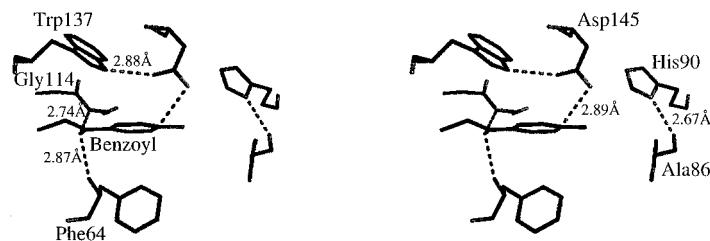


Figure 8. The optimized geometries for the species involved in the hydrolysis with PM3 method.

#### Scheme 4



Trp137 is replaced by phenylalanine, the turnover rate of the mutant enzyme is about 60-fold slower than that of ( $k_{\text{cat}}$ ) wild-type dehalogenase.<sup>10b</sup> Clearly, the loss of the hydrogen bond that holds the carboxylate of Asp145 in the right orientation is responsible for the reduced activity of the mutant enzyme. In the Trp137Phe mutant, the side chain carboxylate of the Asp145 becomes much less restricted in exploring conformations other than the NAC; therefore, the mole fraction of the NACs would be substantially reduced compared to those of the wild-type enzyme.

A similar strategy seems to be employed by glutathione *S*-transferases, a class of enzymes that catalyze the nucleophilic conjugation of a tripeptide glutathione (GSH or HSG) to a large number of compounds that contain an electrophilic group.<sup>40</sup> It is generally believed that the role of the hydroxyl group of the active site tyrosine (or serine in  $\theta$  class of GSTs and tetrachloroquinone dehalogenase) is to facilitate the generation of thiolate from GSH by stabilizing the thiolate through hydrogen bonding.<sup>40</sup> Replacement of the active site tyrosine by phenylalanine in a  $\mu$  class of enzyme shifts the  $\text{p}K_{\text{a}}$  of the enzyme bound GSH to 7.8 from 6.2 of the wild-type enzyme. Since the  $\beta_{\text{nuc}}$  is positive, according to normal Brønsted behavior of a thiolate nucleophile, the mutant enzyme should have a higher

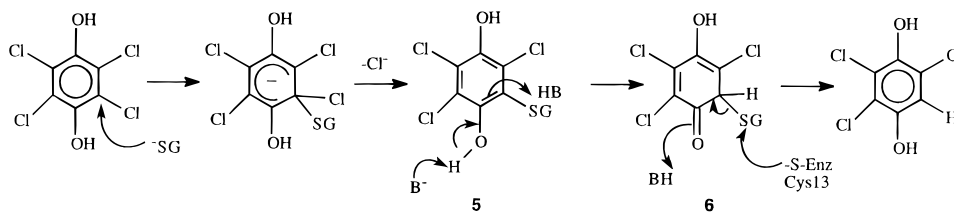
reactivity at higher pH. However, experimental data show that at high pH the reactivity of the mutant is actually less than that of the wild-type enzyme. This abnormal behavior remains an unresolved question.<sup>40</sup> One simple explanation is that the active site tyrosine plays an additional role of orienting the nucleophile (thiolate) and the electrophile in the right orientation (like a NAC) to allow chemical reaction to occur. Removal of this hydrogen-bonding interaction in the mutant will disrupt the NAC arrangement, therefore, causing a reduction in activity. Although the nucleophile (thiolate) is more basic in the mutant enzyme, the relative orientation of the nucleophile to the electrophile is also important for reaction and the latter factor overcompensates the former. The crystal structure of the ternary complex of GST-GS<sup>-</sup>-substrate is presently not available. If this structure does become available, it is expected to retain the relative orientation of GS<sup>-</sup> to the electrophile in a conformation expected for a "NAC".

Returning to the 4-chlorobenzoyl CoA dehalogenase (Scheme 4), the carbonyl oxygen of the thioester moiety is hydrogen bonded to amide hydrogens of Phe64 and Gly114; the hydrogen-bonding distances (O $\cdots$ N) are 2.9 and 2.7 Å, respectively. Although these two hydrogen bonds are not very strong in the reactant, they become much stronger in the transition state (or the Meisenheimer intermediate) because of the developing negative charge at the carbonyl oxygen of the thioester as the

(40) Armstrong, R. N. *Adv. Enzymol. Relat. Areas Mol. Biol.* **1994**, *69*, 1.



## Scheme 5



reaction proceeds. This “differential” hydrogen bonding will certainly speed up the enzymatic reaction.

Another point which was not appreciated before is the fact that the proper orientation of His90 is apparently maintained by a hydrogen-bonding interaction between N $\delta$ -H of the imidazole ring of His90 and the main chain oxygen of Ala86 with a hydrogen bonding distance (O $\cdots$ N) of 2.7 Å, which resembles a recent report on the *Streptomyces scabies* esterase.<sup>37b</sup> In the esterase, the active site His is held in the correct orientation by a neutral hydrogen bond as opposed to the ionic hydrogen bond (Asp $\cdots$ His) in chymotrypsin-like catalytic triads. 4-Chlorobenzoyl CoA dehalogenase appears to be another such case.

**Dehalogenation of Tetrachloroquinone.** Recently, there has been considerable interest concerning the enzyme involved in the biodehalogenation of tetrachloroquinone.<sup>30</sup> Tetrachloroquinone dehalogenase catalyzes the reductive dehalogenation of tetrachloroquinone. This dehalogenase seems to be related to members of glutathione *S*-transferase (GST) superfamily, especially the  $\theta$  subclass of GSTs. Although, there are still many unanswered questions regarding the catalytic reaction mechanism, one of the proposed pathways involves an initial nucleophilic aromatic substitution process (Scheme 5).<sup>30d</sup> In relating the present study to this system, we carried out PM3 calculations for the initial nucleophilic aromatic substitution reaction between tetrachloroquinone and glutathione (as modeled by thiomethoxide).

The calculated potential energy surface in the gas phase is depicted in Figure 9. The gas phase reaction profile resembles both the reaction between 4-Cl-Ph-CO-SCH<sub>3</sub> and CH<sub>3</sub>COO<sup>-</sup> and the reaction between CDNB and thiomethoxide, but no minimum corresponding to the Meisenheimer intermediate was found for the reaction between tetrachloroquinone and glutathione (thiomethoxide). This later reaction seems to be concerted and involves no intermediate. The reactant-side ion-molecule complex (RC) is a hydrogen-bonded complex; the hydrogen-bonding distance (H $\cdots$ S) is about 1.77 Å (Figure 10). In the transition state, the S $\cdots$ C distance is about 2.58 Å and the C-Cl distance is 1.71 Å, indicating an early transition state.

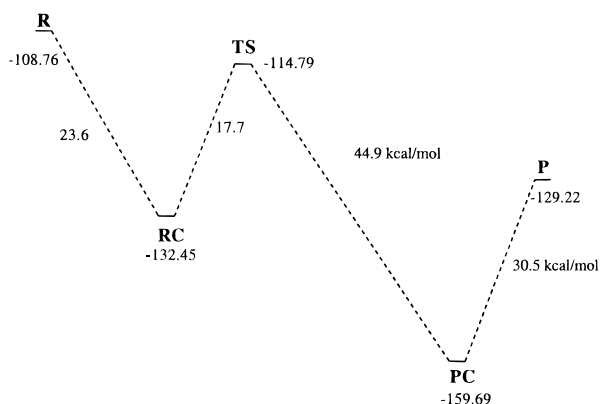


**Figure 9.** The calculated potential energy surface for the nucleophilic aromatic substitution reaction between tetrachloroquinone and glutathione (as modeled by thiomethoxide) with PM3 method.

In the product-side ion-molecule complex (PC), chloride ion forms a strong hydrogen bond with one of hydroxyl hydrogens and a weak one with one of the methyl hydrogens. The presence of this chloride ion polarizes the hydroxyl group, making the carbon to which the -SCH<sub>3</sub> group is attached more like a carbanion. This seems to provide a way to the tautomerization (via deprotonation/protonation) as required by the proposed mechanism (see Scheme 5).

As shown in Scheme 5, tautomerization of 5 to 6 is an important feature of the proposed reaction mechanism. According to our calculations, 6 is about 16.6 kcal/mol higher in energy than 5 and the tautomerization is endothermic.

## Conclusions

To gain a deeper understanding of the catalytic mechanism of 4-chlorobenzoyl CoA dehalogenase catalyzed dehalogenation of 4-chlorobenzoyl CoA to 4-hydroxybenzoyl CoA, the uncatalyzed reaction was investigated in detail both in gas phase and in solution using quantum mechanics method in combination with a self-consistent continuum solvent model. The gas phase nucleophilic aromatic substitution reaction between 4-Cl-Ph-CO-SCH<sub>3</sub> and CH<sub>3</sub>COO<sup>-</sup> is exothermic, with small activation barrier (the overall potential energy barrier is 4.9 kcal/mol at the B3LYP/6-311+G\*\* level of theory). The calculated ab initio reaction profile is best described by a two-well potential surface, with the two potential wells corresponding to reactant-side and product-side ion-molecule complexes. The semiempirical molecular orbital calculations with the PM3 method were able to closely reproduce the B3LYP/6-311+G\*\* results, indicating that PM3 could be used to investigate this kind of reaction in the active site of enzymes. On the PM3 potential energy surface, there is a very shallow minimum that corresponds to the Meisenheimer intermediate. It is likely that the Meisenheimer intermediate could become much more stable in solution or in the active site where the negative charge in the Meisenheimer intermediate can be effectively stabilized by the amide hydrogens of Phe64 and Gly114. A reaction profile in solution was also calculated using the PM3-SM3 method developed by Cramer and Truhlar.<sup>22</sup> According to these calculations, the two ion-molecule complexes are not minima on the potential energy surface in solution, which is expected. There is also a large barrier for this nucleophilic aromatic substitution reaction in solution, and the free energy barrier calculated with PM3-SM3 model is about 37.4 kcal/mol.

Several factors that controls the catalytic power of this dehalogenase have been discussed on the basis of the present study of the uncatalyzed reaction as well as the recent X-ray crystallographic<sup>9</sup> and mutagenesis studies.<sup>10</sup> First, it was proposed that one way to speed up this nucleophilic aromatic substitution reaction is to provide a nonaqueous environment where the chemical reaction is segregated from the solvent and can occur rapidly. Second, the active site Trp137 holds the nucleophile (the carboxylate group of Asp145) via a hydrogen-bonding interaction in an orientation relative to the benzoyl ring, such that the benzoyl ring and the nucleophile are in a “near attack conformation” (NAC). A previous study has demon-

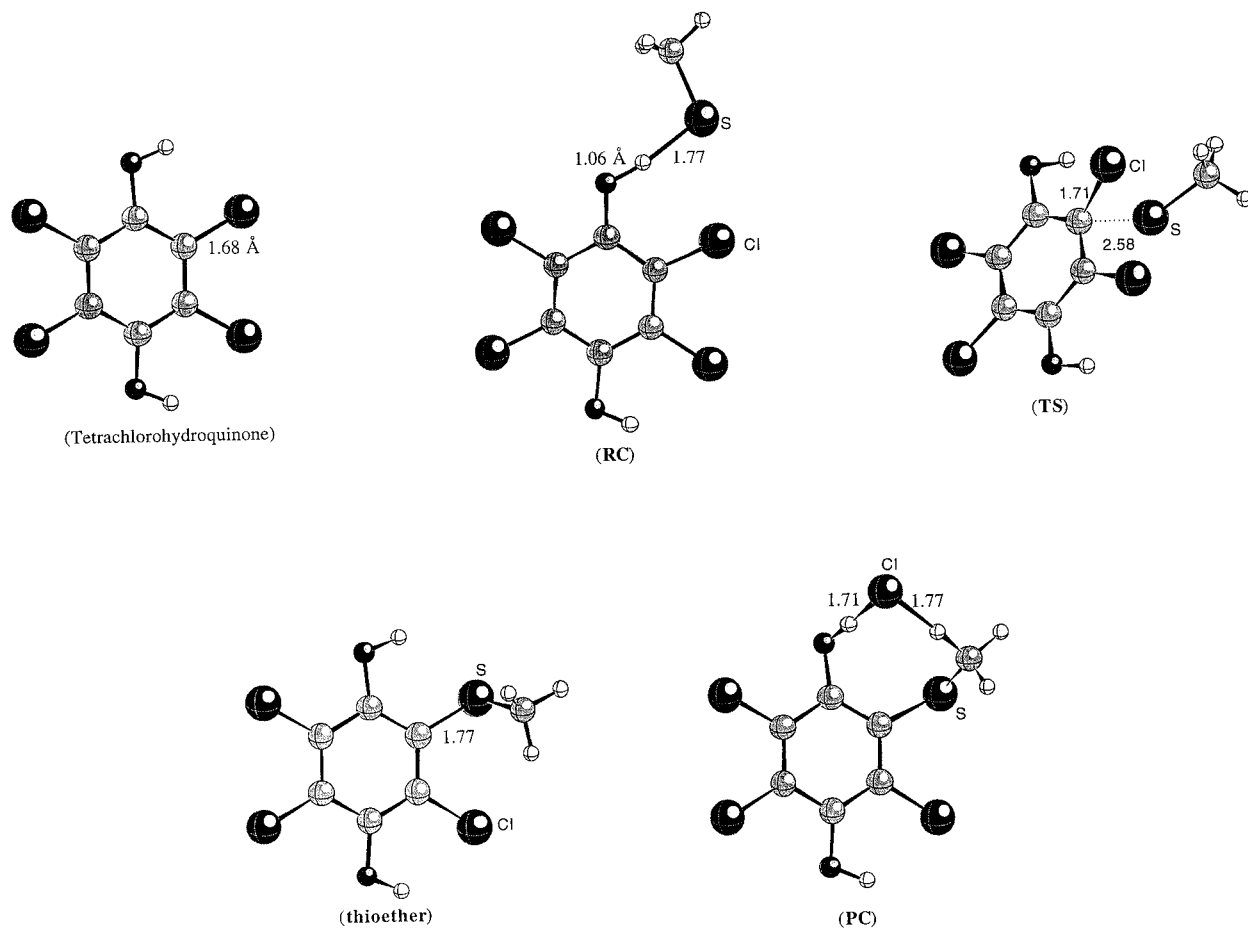


**Figure 10.** The optimized geometries for species involved in the nucleophilic aromatic substitution reaction between tetrachlorohydroquinone and glutathione (as modeled by thiomethoxide) with PM3 method.

strated the relationship between the rate of reaction and the fraction of conformations that are NACs.<sup>39</sup> Disruption of this interaction by replacing Trp137 with phenylalanine, will reduce the mole fraction of NAC, resulting in reduction of catalytic efficacy of the enzyme, as shown experimentally.<sup>10</sup> Third, as revealed by X-ray crystal structure,<sup>9</sup> there are two hydrogen bonds between the carbonyl oxygen of the thioester moiety and the amide hydrogens of Phe64 and Gly114. These two hydrogen bonds become stronger as reaction proceeds due to accumulation of a negative charge upon what was an ester carbonyl oxygen. This “differential” hydrogen bonding will reduce the reaction barrier of the enzymatic reaction. Finally, according to the X-ray crystal structure,<sup>9</sup> the proper orientation of the active site His90 is maintained by a neutral hydrogen-bonding interaction between N $\delta$ -H of the imidazole ring of His90 and the main chain oxygen of Ala86.

We also examined the dehalogenation reaction of tetrachlorohydroquinone. According to our PM3 calculations, the

reaction between tetrachlorohydroquinone and glutathione (as modeled by thiomethoxide) is concerted in the gas phase. Apart from stabilizing the thiolate anion, an additional role of the active site Tyr of glutathione *S*-transferase (or Ser in the  $\theta$  subclass of GSTs and tetrachlorohydroquinone dehalogenase) is to orient the nucleophile (thiolate) and the electrophile in a right orientation to allow chemical reaction to occur.

**Acknowledgment.** We thank Professor Hazel M. Holden (University of Wisconsin) for providing us with the X-ray coordinates of 4-chlorobenzoyl CoA dehalogenase and Professor Debra Dunaway-Mariano for sharing with us their new experimental data. We also thank the referees for their suggestions. The support of NCSA for computing resource is also appreciated. This study was supported by National Institute of Health and National Science Foundation.

JA970114J